# Comparative Effects of Lipid Transfection Reagents on Transfection Efficiency and IL-1 Cytokine Induction in H1299 Cells

Kevin Aby, Armaan Balani, Zachary Caldera, Jake Caravello, Sophie Gang, Christine Johansen, Megan Kim, Kabir Kalsi, Stephanie Liao, Sam Rosen, Tianyi Iris Shen, Anya Verma

Advisor: Dr. Brianne Barker
Assistants: Brenna Hezel, Emily Shirk

## ABSTRACT

Lipid-based transfection systems are widely used to deliver nucleic acids directly into cells, yet its effect on innate immune responses is still poorly understood. Host innate immune pathways recognize foreign biomolecules, often categorized as microbe-associated molecular patterns (MAMPs), via pattern recognition receptors (PRRs) and restrict transgene expression. While previous research has primarily focused on nucleic acid-mediated innate immune activation, emerging evidence suggests that lipid transfection carriers themselves may also stimulate innate immune signaling. However, the underlying mechanisms—how commercial lipid reagents differ in inducing inflammatory cytokine cascades independent of nucleic acid delivery—remain unclear. We evaluated whether different commercial transfection carriers trigger intrinsic IL-1 family cytokine responses independently of nucleic acid cargo, and whether this response varies across reagents. H1299 cells were treated with Lipofectamine 2000 and Polyethylenimine (PEI) in the presence and absence of plasmid DNA. Transfection efficiency was quantified via ampicillin-resistance (ampR) gene delivery, and immune activation was measured using qPCR for IL-1α and IL-1β.

Both reagents induced significant cytokine expression even in the absence of DNA, showing that delivery vehicles activate innate immune pathways. However, Lipofectamine 2000 achieved a higher transfection efficiency while inducing a significantly weaker inflammatory response compared to PEI. When combined with DNA, PEI vastly upregulated IL-1α and IL-1ß. These findings show that the chemical composition of the delivery particle plays a significant role in determining cellular response. Therefore, understanding each reagents' individual DNA transfection rate and the reagent-induced innate immune cytokine response cascade is critical for designing transfection reagents tailored for specific therapeutic applications, such as minimizing innate immune inflammation for gene therapies or using it to strengthen vaccine-induced immunity.

## INTRODUCTION

In recent years, nucleic acid vaccines have revolutionized disease treatment and prevention through intracellular transfection of mRNA and DNA. DNA vaccines typically use plasmids, circular DNA molecules that encode the target antigen, and must enter the nucleus before transcription can occur. In contrast, mRNA vaccines deliver messenger RNA directly to the cytoplasm, where it is translated into protein. While viral vectors achieve high transfection efficiency, their implementation is constrained by safety risks, such as unwanted immune responses from with adeno-associated viruses (Tsaregorodtseva et al., 2026) and high manufacturing costs (Thakur et al., 2024). Non-viral, lipid-based delivery systems offer a significantly safer, more scalable, and cost-effective alternative. However, their main bottleneck remains lower overall transfection efficiency. Host innate immune responses detect a large range

of microbe-associated molecular patterns (MAMPs), activating antiviral signaling pathways that produce inflammatory cytokine cascades and, based on the pathways involved, may establish an antiviral state capable of suppressing transgene expression (Warga et al., 2023). Yet, questions remain how reagents contribute to immune activation. The interaction between transfection reagents and PRRs is hypothetical. There is no insight into which PRRs may be getting activated by these reagents, or even if PRRs are activated by individual reagents. This uncertainty is only further cemented by proprietary formulations and the relative recency with which PRRs were discovered. For these reasons, identifying possible mechanisms by which transfection reagents activate PRRs is beyond the scope of this study.

Innate immune activation by nucleic acid delivery systems is primarily driven by pattern recognition receptors (PRRs). There are many different types of PRRs such as endosomal Toll-like receptors (TLRs), RIG-I-like Receptors (RLRs), and C-type Lectin Receptors (CLRs). Their role is to detect conserved molecular patterns associated with pathogens–commonly referred to as microbe-associated molecular patterns (MAMPs)-- including foreign nucleic acids. Once activated, PRRs initiate inflammatory signaling characterized by the production of cytokines and type I interferons (Barber, 2015). Given their role in detecting foreign material, the proposal that certain transfection reagents may also activate PRRs is a reasonable argument. For the purposes of this study, many PRRs are vital to the expression of these cytokines including certain TLRs, cGAS, and IFI16 to detect the DNA plasmid and induce inflammatory signaling cascades that produce a broad inflammatory response. In order to measure the outcomes of these PRRs, this study specifically focuses on cytokines *IL-1α* and *IL-1β*, two pro-inflammatory cytokines that have been overlooked in the transfection literature despite evidence tying them into lipid-associated innate immune activation (Tahtinen et al., 2022).

While nucleic acids have been identified as notable stimuli for innate immune activation during transfection, PRRs have the capability to recognize a wide variety of molecular structures encompassing all MAMPs. Consequently, it is biologically plausible that reagent-based delivery systems may also be at the rein of engaging innate immune sensing pathways. To further back up this claim, emerging evidence demonstrates that lipid deliveries are not merely inert (Warga et al., 2023; Tahtinen et al., 2022). Rather, certain findings suggest that the lipid itself independently activates the innate immune signaling and the ensuing inflammatory cascade, effectively allowing the lipid to trigger the synthesis of cytokines even in the absence of RNA or DNA (Tahtinen, 2022).

Previous studies, such as Tahtinen and colleagues, have suggested that variations within reagents' chemical structure and properties contribute to differences in both transfection efficiency and the strength of the inflammatory pathway activation. Despite similar biodistribution patterns, researchers have been able to prove that different lipid nanoparticles (LNPs) can produce distinct transfection outcomes (Wei et al., 2026). Tahtinen et al. compared the effects that four LNPs have on trafficking and transfection in major organs. These findings were obtained using mouse models and different LNPs than those being used in this study. However, they support the broader assertion that the different chemical composition of each lipid is a critical factor in inducing varying levels of transfection efficiency and should be evaluated independently for each delivery system (Tahtinen et al., 2022). Tahtinen and colleagues have pointed out that the innate immune responses to transfection reagents differs between mouse and

human cells. Due to such interspecies discrepancies in the innate immune system, conclusions drawn from mouse models cannot be directly translated from mouse data to human data. Although many of the trends found by Tahtinen et al. in mouse cells are expected to also be found in human cells, this must still be experimentally validated. Therefore, H1299 cells were selected as a human cellular model to evaluate whether different lipid transfection reagents produce similar effects on plasmid uptake and *IL-1α* and *IL-1β* expression. To our knowledge, It has not been previously studied whether commercially available lipid reagents differ in induced *IL-1α* and *IL-1β* expression in human cells. Given Tahtinen et al.'s findings that Il-1 cytokines may contribute to the side effects of LNP-delivered RNA vaccines and that these responses differ between mouse and human cells, evaluating these cytokines in a human model represents an important gap in the current literature.

The purpose of this experiment was to compare the relative plasmid delivery and innate immune activation profiles of different transfection reagents, providing scientists with an initial framework to select a reagent based on the desired balance between transfection and innate immune activation. Based on the intended application, such as gene therapy or vaccine development, the optimal balance between these outcomes may differ. Therefore, other researchers can use the findings from this study as the foundation for future investigations for selecting reagents based on the desired balance between delivery efficiency and immune stimulation.

To distinguish the effects of the lipid carrier from those driven by the nucleic acid, our study utilizes an experimental design featuring conditions both with and without plasmid DNA to isolate these distinct effects. To evaluate this experimentally, human H1299 cells were transfected with plasmid DNA using two different transfection reagents. Following transfection, DNA and RNA were harvested from each treatment group. Quantitative PCR (qPCR) was performed on extracted DNA to quantify plasmid uptake by measuring the copy number of the ampicillin resistance (*ampR*) gene, while reverse transcription quantitative PCR was used on extracted RNA to quantify *IL-1α* and *IL-1β* gene expression. The culmination of our qPCR values came to fruition in a fold change value. Fold change in ampR served as a measure of plasmid uptake, while fold changes in L-1α and IL-1β reflected innate immune activation. Together, these outcomes allowed direct comparison of the relative delivery and inflammatory profiles of the different transfection reagents. Based on this rationale, we hypothesized that each transfection reagent will elicit varying levels of cytokine release rather than directly correlating with the amount of DNA transfected due to reagent-induced innate immune responses.

## METHODS

Cell Preparation

H1299 cells, a line of epithelial-like cells derived from the lung carcinoma of a 43 year old man, were cultured in R10 medium (RPMI media, 10% fetal bovine serum, 5 mL/500 mL penicillin-streptomycin-glutamine (PSG), 5 mL/500 mL sodium pyruvate, 5 mL/500 mL HEPES buffer, and 5 mL/500 mL 7.5% sodium bicarbonate. Cells were incubated overnight at 37°C and 5% $CO_2$.

Cell Stimulation

Cells were plated in a 12 well plate, each containing $5x10^5$ cells cultured in 1mL R10 media composed of RPMI (Roswell Park Memorial Institute) and 10% other components including L-glutamine, sodium bicarbonate, HEPES, and sodium pyruvate. Trypan Blue Dye was used to clearly identify and count cells with a hemocytometer. The well plates were then cultured in an incubator kept at 37℃ and 5% $CO_2$ for 48 hours to replicate the internal conditions of the human body. After the H1299 cells were incubated for 48 hours, cells were stimulated and transfected using various lipids and DNA (Figure 1). 3 tubes were prepared, labelled A-C. Tubes A and B each contained 288µL of Opti-MEM media (Opti) and, in tube A, 12 µL Lipofectamine, and in tube B, PEI. Tube C contained 300 µL of Opti. Next, 6 tubes were prepared, labelled 1-6. Tubes 1-3 each contained 100 µL of Opti and, in order, 100 µL of tubes A-C. Tubes 4-6 each contained 62 µL of Opti, 38 µL (6.25 ng/µL) pcDNA3-EGFP solution (Figure 2), and, in order, 100 µL of tubes A-C. The tubes then rested for 20 minutes to allow for liposomes to form around DNA fragments in the tubes containing DNA. The contents of the tubes 1-6 each were split into 2 cell wells, each given 100 µL of the total 200 µL tube. The plate was then incubated at 37℃ and 5% $CO_2$ for 72 hours.

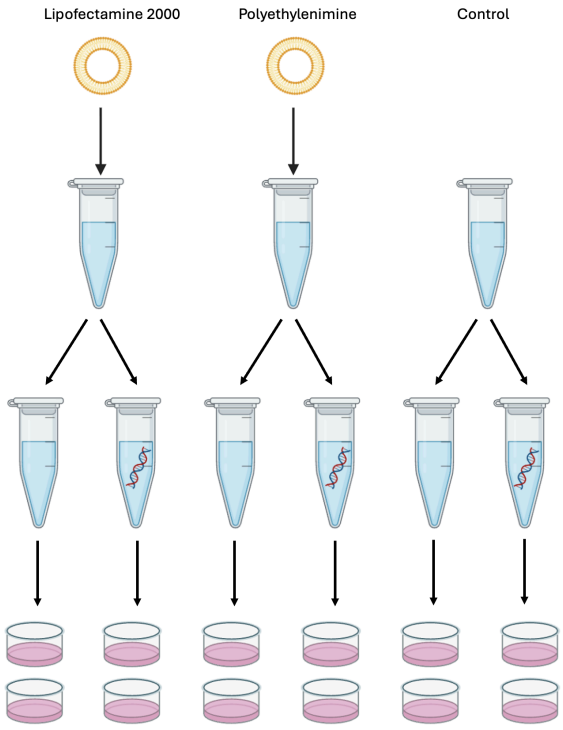



***Figure 1*. Cell Stimulation Visual.** First, 12 µL of each transfection reagent (Lipofectamine 2000 and polyethylenimine [PEI]) was added to 288µL of Opti-MEM, serum-free transfection media, while the control microcentrifuge tube contained 300µL of Opti-MEM alone. Next, 100µL of each lipid mixture was transferred into two microcentrifuge tubes: one set containing 100 µL of Opti-MEM alone and the other containing Opti-MEM with 200 ng of DNA for a total volume of 100µL. The resulting mixtures were incubated for 20 minutes before being divided equally between two wells, with 100 µL added to each well.

Nucleic Acid Extraction

Following incubation, the contents of each well were centrifuged at 500xg for 5 minutes. The supernatant was discarded and the remaining pellet disrupted and mixed with 200 µL of phosphate-buffered saline solution (PBS). Then, each 200 µL tube was split into two identical 100 µL tubes to allow for measurements of both DNA plasmid and transcribed RNA from each well. Immediately following this split, all tubes for DNA testing were set on ice during RNA extraction.

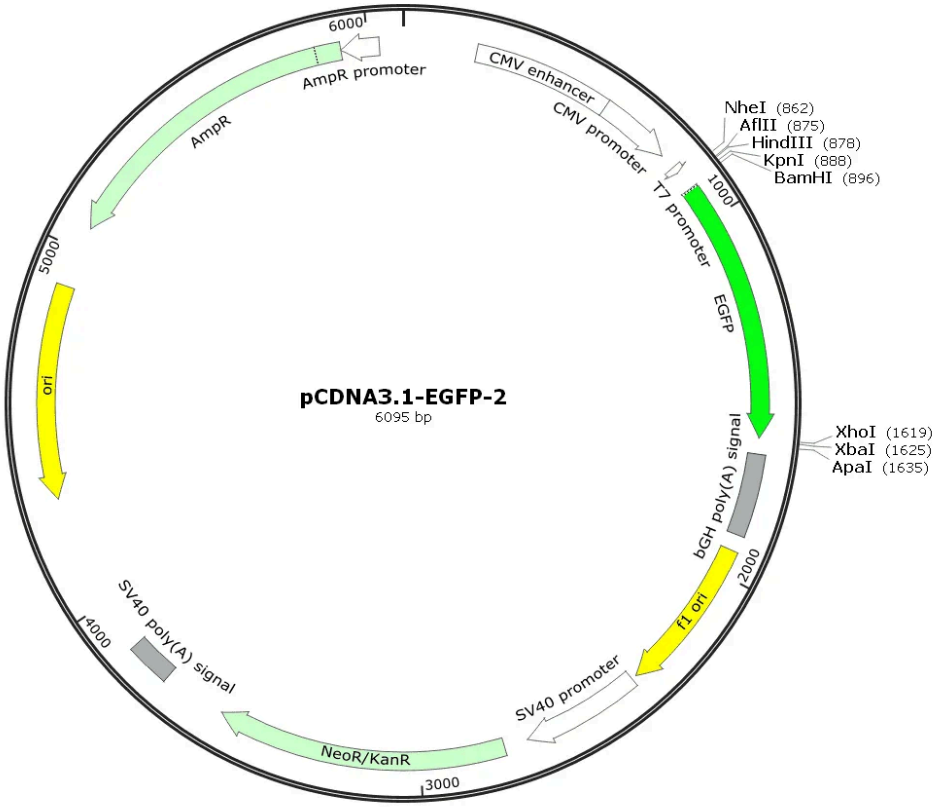



***Figure 2.*** **Genes contained in pcDNA3-EGFP.** Note an ampicillin resistance gene is included, which is what will be measured to confirm transfection by qPCR.

RNA Extraction

In accordance with the procedure specified in New England Biolabs Monarch Spin RNA Isolation Kit, the following steps were taken to extract RNA from the cells. First the RNA tubes were centrifuged at 500xg for 5 minutes to remove the PBS,, and the pellet was resuspended in 350 µL of Monarch StabiLyse lysis buffer to lyse the cell, release the RNA, and denature the RNase present. Each tube's contents were then centrifuged at 1600g for 1 minute in S2C spin columns so the DNA present would adhere to the matrix and be removed. After discarding the column, an equal volume (350 µL) of 95% ethanol was added to each tube, disrupting the RNA's hydration shell and allowing the present positively charged salt to neutralize the negative RNA. With the RNA now neutral, it binds to the silica matrix of an S2A Spin column upon another round of centrifugation at 16000xg for 1 minute. The flow-through was removed and 700 µL of ethanol-based Monarch Buffer WZ was added to remove salts and other contaminants from the

RNA through centrifugation at 16000xg for 1 minute. The flow-through was again removed and 80 µL of DNase mixture (86% reaction buffer, 14% DNase 1) was added to each column to destroy any residual DNA. Then, all tubes were incubated for 15 minutes at room temperature.

500 µL of Monarch Buffer BX was added to each tube after incubation to remove the DNase mixture and prime the silica matrix to preserve RNA. Each tube was then centrifuged at 16000xg for 1 minute. The flow-through was discarded and 500 µL of Monarch Buffer WZ was added to remove any remaining contaminants. An identical centrifugation procedure and flow-through removal was performed before another 500 µL of Monarch Buffer WZ was added to each tube. This time, however, centrifugation at 16000xg was performed for 2 minutes to dry the silica matrix, removing residual ethanol. The collection tubes were then replaced with a 1.5 mL microfuge tube. 40 µL of nuclease-free water was then added directly to each column and incubated at room temperature for 3-5 minutes before a final centrifugation at 16000xg for 30 seconds. The RNA, now purified in the microfuge tube, was placed on ice to minimize RNase activity.

DNA Extraction

Similar to the technique used for RNA extraction, adherence to New England Biolab's Monarch Spin gDNA Extraction Kit allowed for the purification of DNA from the cells. After resuspending the cell pellet, 1µL of Proteinase K and 3µL of RNase A were added and dispersed through vortexing. Cell lysis was initiated by adding 100µL of Cell Lysis Buffer, followed immediately by thorough vortexing until the lysate became viscous. The mixture was incubated at 56°C for 5 minutes with intermittent vortexing. Then, 400µL of gDNA Binding Buffer was added and vortexed, and the resulting mixture was transferred to a Monarch Spin Column S2C fitted into a collection tube and centrifuged at 16300xg for 1 minute. The column was transferred to a fresh collection tube, and 500µL of gDNA Wash Buffer was added. The tube was inverted several times to wash the column cap, then centrifuged immediately at 16300xg for 1 minute before discarding the flow-through. This wash was repeated once more and the spin column was placed into a microcentrifuge tube. To elute the gDNA, 100µL of preheated 60°C gDNA Elution Buffer was added to the column. and incubated at room temperature for 1 minute, before centrifugation 17000xg for 1 minute. The spin column was discarded, and the eluted gDNA was immediately placed on ice.

cDNA Synthesis

cDNA (complementary DNA) synthesis materials and procedures were adapted from a New England Biolabs ProtoScript II First Strand cDNA Synthesis kit. cDNA synthesis is necessary to allow qPCR, as the 90ºC stage of PCR is hot enough to break down RNA, whereas DNA is stable enough to survive it. From each of the tubes, 6 µL of RNA sample was added to an empty microtube with 2 µL of 50 µM Oligo(dT) primer and denatured in a 50ºC heat block for 5 minutes. The tubes were then placed immediately on ice for 30 seconds before centrifugation at 16300xg for 100 seconds and being returned to ice. To each tube, 10 µL of Protoscript II Reaction Mix and 2 µL of Protoscript Enzyme Mix were added and allowed to incubate at 42ºC for 1 hour. Finally, the tubes were incubated at 80ºC for 5 minutes before storage at -20ºC.

qPCR Reactions

To measure the cytokine production and transfection efficiency, qPCR (quantitative polymerase chain reaction) was performed on the cDNA and DNA samples respectively using a Bio-Rad CFX96 Real-Time PCR Detection System. Quantitative PCR was identified as the ideal method for gathering data as opposed to standard PCR because qPCR allows for the gathering of data during amplicon amplification. To quantify the products of the PCR reaction, SYBR green, a green fluorescent marker, was used. SYBR Green binds to double stranded DNA and is sensed during each cycle of exponential DNA replication, giving an accurate reading of the amount of double stranded DNA present at the end of each PCR reaction. For both cDNA and DNA qPCR reactions, the primer RPL37A was used as a control because it displays constant expression in all cells, coding for a consistently produced protein in the ribosome.

***Table I*: qPCR Primer Sequences**

| **qPCR Primer (Forward)** | **Sequence** | **qPCR Primer (Reverse)** | **Sequence** |
|---|---|---|---|
| IL-1b Forward | ATGGACAAGCTGAGGAAGATG | IL-1b Reverse | CCCATGTGTCGAAGAAGATAGG |
| IL-1a Forward | TGTATGTGACTGCCCAAGATGAAG | IL-1a Reverse | AGAGGAGGTTGGTCTCACTACC |
| Ampicillin (plasmid) Forward | TCCGGTTCCCAACGATCAAG | Ampicillin (plasmid) Reverse | AGTGATAACACTGCGGCCAA |

To quantitate the RPL37A, IL-1a, and IL-1b transcripts in the cDNA samples of H1299 cells, qPCR reactions were set up. Each qPCR reaction contained 10µL of SYBR Green, 1µL of Forward Primer, 1µL of Reverse Primer, 1µL of cDNA sample, and 7µL of DNAse-free water. Similarly, qPCR was used to quantitate the amount of Ampicillin and RPL37A in the DNA samples of H1299 cells. Each reaction contained 10µL of SYBR Green, 1µL of Forward Primer, 1µL of Reverse Primer, 1µL of DNA sample, and 7µL of DNAse-free water.

All qPCR reactions began with an initial 3-minute 95°C denaturation period to separate the hydrogen bonds in the DNA. This was followed by 40 cycles, each consisting of 10 seconds of 95°C denaturation and 30 seconds of 60°C annealing and elongation, during which the forward and reverse primers annealed to the target DNA and DNA polymerase synthesized the complementary strands. Then, the melt curve analysis was performed by heating the samples from 65°C to 95°C in 0.5°C increments in order to verify the specificity of the amplification.

Data Analysis

For each qPCR sample tested, a CQ (quantification cycle) was recorded. This value represents the cycle number at which the level of DNA crossed a critical threshold of exponential growth. However, because different samples can have different starting amounts of DNA, the RPL37A control was taken into account to provide a ΔCQ value that measured the amount of target DNA relative to the total quantity of DNA (Livak, 2001). For all ΔCQ calculations, 20 was used as the CQ for RPL37A, a typical expected value for RPL37A in this lab with this procedure (*Poremba, 2017*).

$$\Delta CQ = CQ - CQ_{avg\ RPL37A} \quad (1)$$

To measure how the quantity of target DNA in stimulated samples compared to the amount of DNA in unstimulated samples, a ΔΔCq value was calculated by comparing to the average ΔCq negative. Cell samples that were not subjected to any stimulation contributed to the average negative ΔCq, which was calculated to be 15.84 for IL-1β and -0.47 for IL-1α.

$$\Delta\Delta CQ = \Delta CQ - \Delta CQ_{avg\ negative} \quad (2)$$

The ΔΔCQ value was used to calculate the fold change for each sample, which gives how many more times a given target gene was expressed relative to the control group (RPL37A). The equation to calculate fold change (FC) is given below.

$$FC = 2^{-\Delta\Delta CQ} \quad (3)$$

Statistical Analysis

Welch's t-test was used to compare the two groups of Lipofectamine and DNA as well as PEI and DNA. It was also used for many other comparisons such as those between lipid only and unstimulated groups. Because this test, unlike the Student's t-test, does not assume that the variance within each group is the same, the number of degrees of freedom for the two groups being tested was calculated using the Welch-Satterthwaite equation (4), as shown below. Note that s represents standard deviation and n represents the number of samples, which is 3. The t-statistic was then calculated by dividing the difference between the means of these two groups by the standard error. This information allowed for the creation of a two-tailed p-value.

$$v = \frac{\left(\frac{s1^2}{n1} + \frac{s2^2}{n2}\right)^2}{\frac{(s1^2/n1)^2}{n1-1} + \frac{(s2^2/n2)^2}{n2-1}} \quad (4)$$

A two-way ANOVA (analysis of variance) test was performed on all samples. The test assesses if the variance in fold change between different groups (Lipofectamine and PEI) is statistically different from the variance within these groups. As a result, it will be possible to determine a statistical difference between the means of the groups. Additionally, it also provides insight into whether the presence of DNA only can affect the FC measured. Finally, the tests show whether the presence of DNA affected the FC of inflammatory cytokines to Lipofectamine samples differently from how it affected PEI samples. ANOVA tests were performed using the Social Science Statistics two-way ANOVA calculator (socscistatistics.com) and Microsoft Excel. A significance threshold of $\alpha = 0.05$ was used throughout.

**RESULTS**

Transfection of the ampicillin-resistance gene (*ampR*) introduced to H1299 via the pcDNA3-EGFP plasmid was measured by qPCR to assess efficacy of plasmid transfection. For Lipofectamine 2000 + DNA, *ampR* transfection was significantly elevated over unstimulated controls ($p = 0.0004$; Welch's t-test on fold change) (Figure 3); PEI + DNA did not reach

significance over unstimulated controls (p = 0.084). DNA with Lipofectamine 2000 produced significantly higher *ampR* transfection than DNA with PEI (p = 0.031).

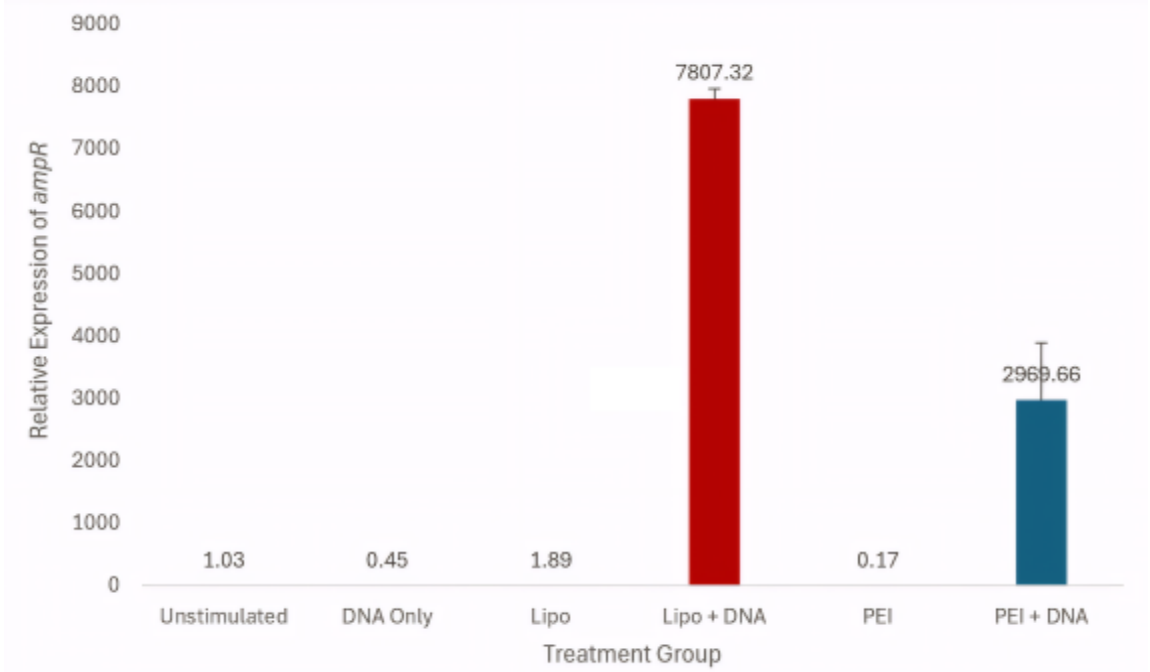



**Figure 3.** ***ampR Transfection Fold Change Bar Graph.*** Shows the fold change for *ampR* Transfection for DNA, Lipofectamine 2000, PEI, Lipofectamine 2000 + DNA, and PEI + DNA in comparison to unstimulated control.

IL-1 Cytokine Induction by Reagent

By themselves, both Lipofectamine 2000 and PEI expressed significantly elevated IL-1α expression relative to unstimulated cells (Lipo: p = 0.0041; PEI: p = 0.0079; Welch's t-test on fold change) and relative to DNA-only controls (Lipo: p = 0.0004; PEI: p = 0.0209; Welch's t-test on fold change) (Figure 4). A similar trend was observed for IL-1β, however a true statistical comparison was not possible due to the lack of replicate data for control wells.

PEI induced higher expression than Lipofectamine for IL-1β and IL-1α both with DNA present (IL-1β: p = 0.057; IL-1α: p = 0.055; Welch's t-test on fold change) and alone (IL-1β: p = 0.193; IL-1α: p = 0.197; Welch's t-test on fold change) (Figures 4, 5). However, none of these comparisons reached significance.

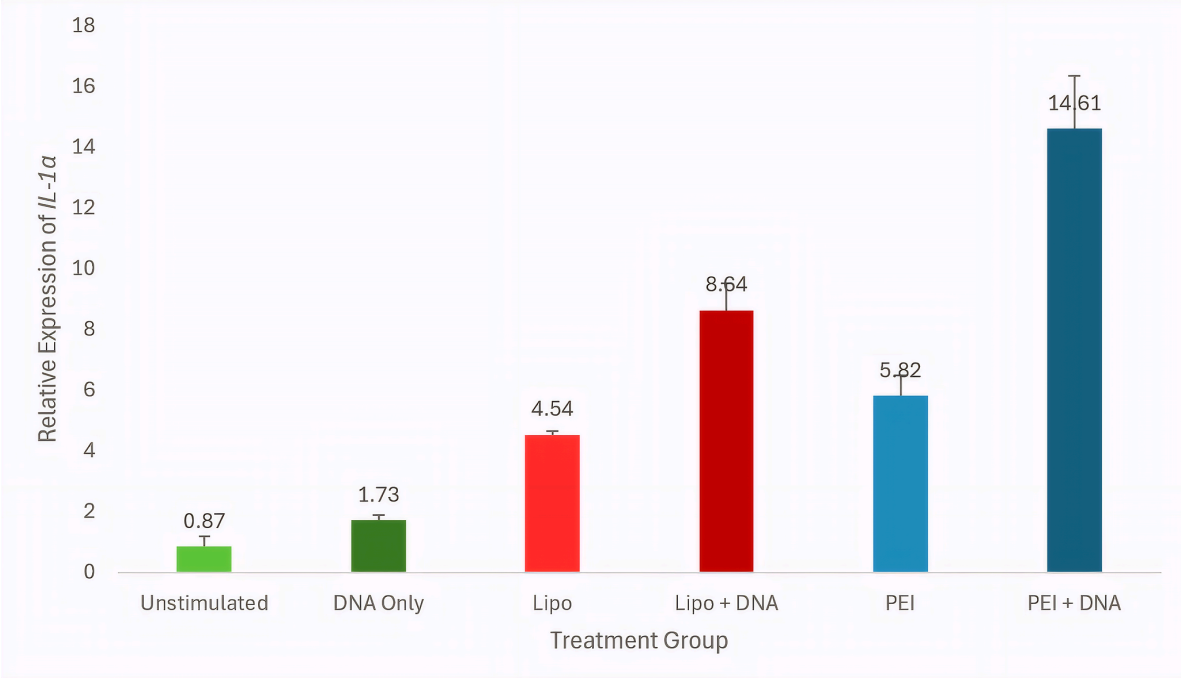



**Figure 4. Cytokine *IL-1α* Expression Fold Change Bar Graph.** Shows the fold change for *ampR* Transfection for DNA, Lipofectamine 2000, PEI, Lipofectamine 2000 + DNA, and PEI + DNA in comparison to unstimulated control.

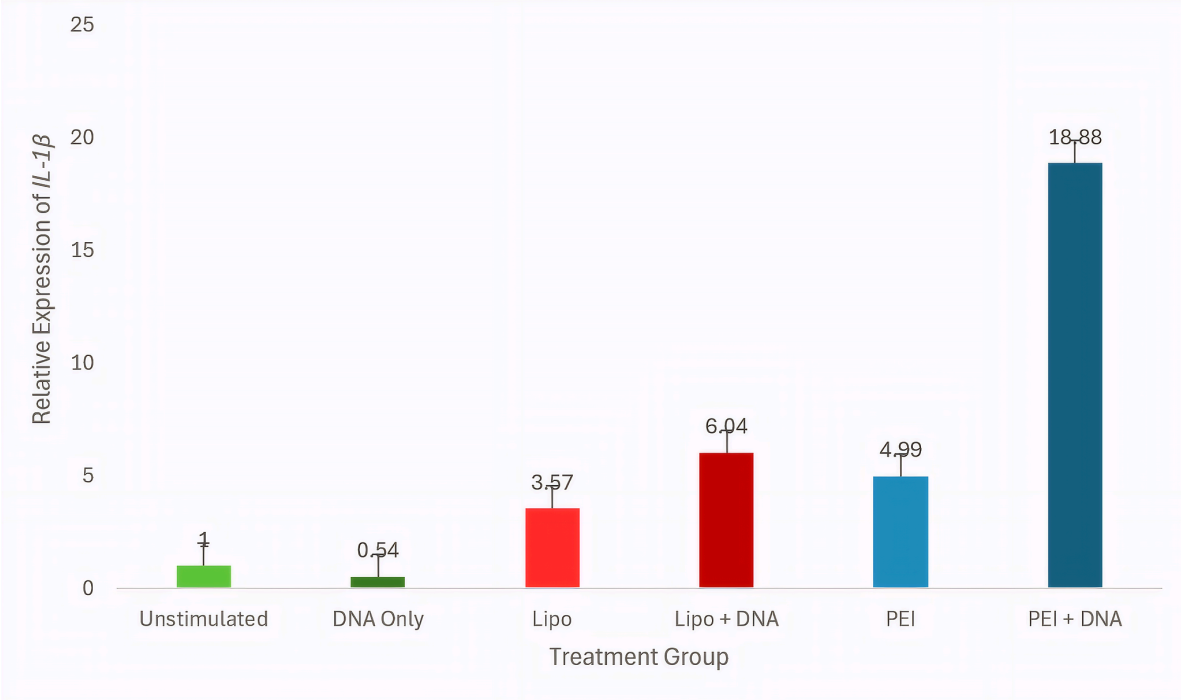



**Figure 5. Cytokine *IL-1β* Expression Fold Change Bar Graph.** Shows the fold change for *ampR* Transfection for DNA, Lipofectamine 2000, PEI, Lipofectamine 2000 + DNA, and PEI + DNA in comparison to unstimulated control.

Combined Effects of Reagent and DNA Presence

Two-way ANOVA (reagent × DNA presence) was performed on fold change values, run separately for IL-1α and IL-1β (Table II, III) for three conditions: whether the lipid used had a significant effect on response without DNA, whether DNA presence affected response regardless of lipid, and whether DNA presence differed depending on lipid.

For IL-1α, both reagent ($F(1,8) = 12.27$, $p = 0.0080$; two-way ANOVA test on fold change) and DNA presence ($F(1,8) = 38.91$, $p = 0.0002$) were significant main effects; the reagent × DNA interaction was not significant ($F(1,8) = 5.15$, $p = 0.0529$) (Table II). For IL-1β, both reagent ($F(1,8) = 16.38$, $p = 0.0037$; two-way ANOVA test on fold change) and DNA presence ($F(1,8) = 21.55$, $p = 0.0017$; two-way ANOVA test on fold change) were significant main effects; the interaction was also significant ($F(1,8) = 10.51$, $p = 0.0118$; two-way ANOVA test on fold change) (Table III).

**Table II: Variance and Statistical Significance of Differences Across Conditions for IL-1α**

| Condition | F | p-value | Significant? |
|---|---|---|---|
| Lone Reagent (Lipo vs PEI) | 12.27 | 0.0080 | Yes |
| DNA (yes vs no) | 38.91 | 0.0002 | Yes |
| Reagent + DNA (Lipo+DNA vs PEI+DNA) | 5.15 | 0.0529 | No |

**Table III: Variance and Statistical Significance of Differences Across Conditions for IL-1β**

| Condition | F | p-value | Significant? |
|---|---|---|---|
| Lone Reagent (Lipo vs PEI) | 16.38 | 0.0037 | Yes |
| DNA (yes vs no) | 21.55 | 0.0017 | Yes |
| Reagent + DNA (Lipo+DNA vs PEI+DNA) | 10.51 | 0.0118 | Yes |

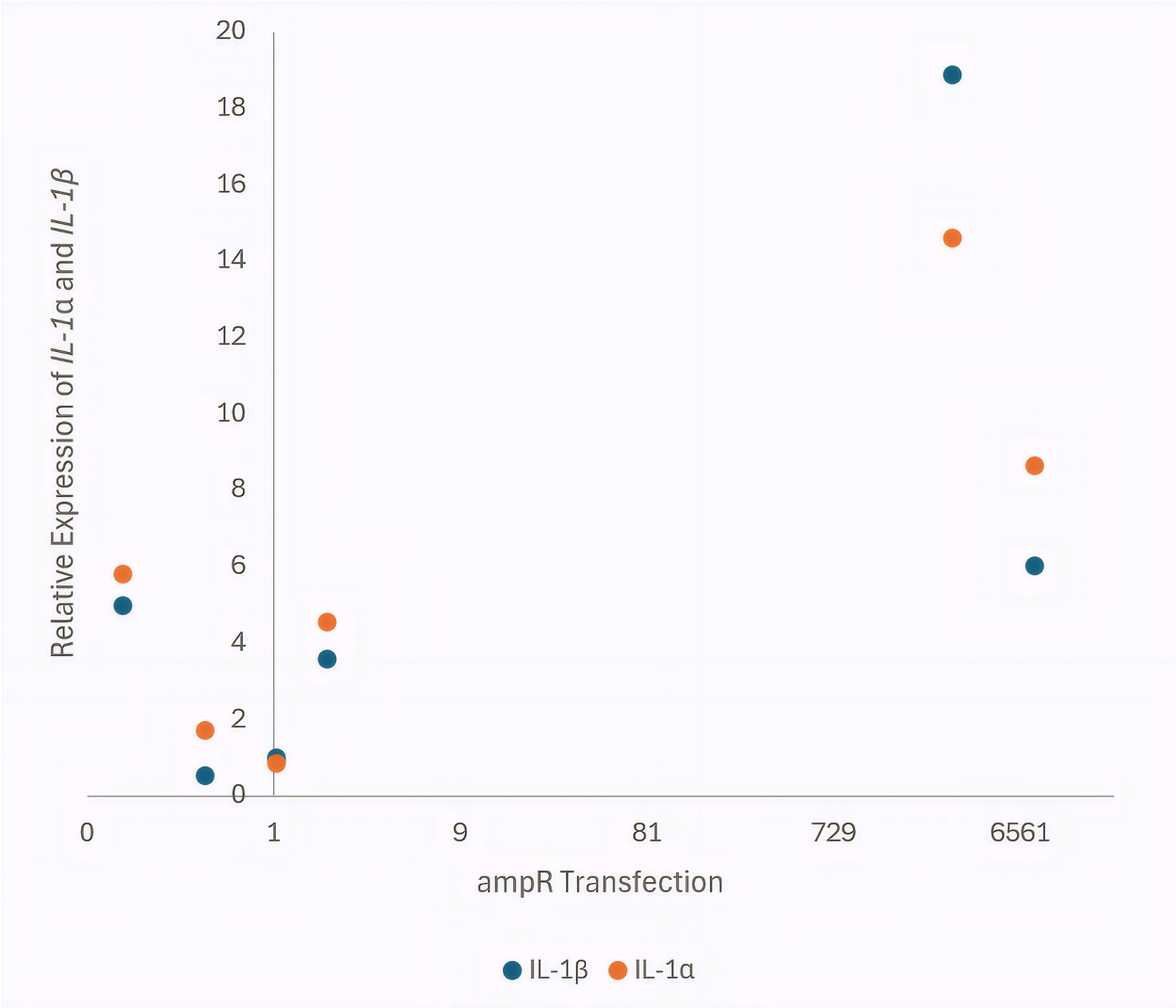



**Figure 6: Relative Expression of *IL-1α* and *IL-1β* Cytokine Expression Versus Relative Transfection of *ampR*.** A logarithmic scale of 3 was used to generate the graph.

*ampR* transfection plotted against IL-1α and IL-1β expression across the four transfected conditions showed Lipo + DNA at the highest *ampR* value paired with the lowest IL-1α/IL-1β values among the DNA-containing conditions; PEI + DNA showed the lowest *ampR* value paired with the highest IL-1α/IL-1β values (Figure 4).

Pearson correlation coefficients were also calculated to assess the relationship between ampR expression and cytokine induction. ampR expression showed a weak to moderate correlation with *IL-1α* (r = 0.38) and a moderate correlation with *IL-1β* (r = 0.57). This suggests that plasmid uptake is only partially predictive of cytokine induction. *IL-1α* and *IL-1β* were themselves strongly correlated with one another (r = 0.96). This is consistent with the earlier findings of little difference between the two cytokines' induction patterns and supports the idea that these related cytokines respond similarly to the same stimuli.

## DISCUSSION

Summary of Key Findings

This study aimed to evaluate the innate immune response in H1299 cells and transfection efficiency of both PEI or Lipofectamine 2000 as the delivery mechanism for the pcDNA3-EGFP plasmid. We hypothesized that cytokine release would vary based on the LNP type, rather than correlating directly with the amount of DNA delivered to the cell. Our findings supported our hypothesis by displaying that not only are LNPs essential for DNA uptake into the cell, but also play a significant role in the scale of resulting innate immune responses.

In order to determine how effectively each LNP delivered plasmid DNA, the presence of plasmid gene *ampR* was measured utilizing qPCR. Lipofectamine 2000 transfected the greatest amount of intracellular *ampR* (Figure 3), indicating that Lipofectamine transfected more DNA into the cell. Each lipid's effect on the innate immune response was quantified by measuring IL-1α and IL-1β expression for each lipid alone and each lipid with DNA transfection. The addition of lipid alone resulted in elevated cytokine levels compared to the unstimulated cells, indicating LNPs' independent modulation of the immune response. Both Lipofectamine alone and Lipofectamine with DNA produced fewer IL-1β cytokines compared to their PEI counterparts (Figure 4, Figure 5).

These findings suggest that Lipofectamine induces a weaker inflammatory response compared to PEI while maintaining higher transfection efficiency, illustrating the LNP's promise in future vaccine development. Nucleic acid vaccines rely on the successful transfection of genetic material, ensuring that the host produces the necessary antibodies to defend against future infection. Lipofectamine's higher transfection efficiency indicates that it would elicit greater host immunity in a nucleic acid vaccine. Lipofectamine's potential for delivering nucleic acid vaccines is further supported by the fact that when transfecting DNA, Lipofectamine caused a reduction in cytokine expression levels compared to PEI with DNA. Based on the statistically significant ANOVA assessment of the differences between IL-1α and IL-1β expression for the two groups, DNA increased fold change substantially more for PEI than for Lipofectamine (Table II, Table III). PEI therefore triggers a greater immune response despite transfecting a lower amount of DNA.

Both types of lipids also independently triggered greater expression of IL-1α and IL-1β compared to the lipid-unstimulated groups (Figure 4, Figure 5). Notably, Lipofectamine alone caused a lower fold change for both IL-1α and IL-1β compared to PEI alone (Figure 4, Figure 5). The baseline expression of cytokines for the unstimulated cells was lower than the fold change of either group with only lipid. The elevated expression of IL-1α and IL-1β without the presence of DNA demonstrates that lipids independently contribute to an intracellular immune response. Additionally, Lipofectamine's lower levels of inflammatory cytokine release compared to that of PEI portray its weaker inflammatory response, suggesting that using Lipofectamine as a transfection agent for nucleic acid vaccines may result in less reactogenicity. As Lipofectamine 2000 is one of the most commonly utilized lipids in laboratory settings, its higher transfection rate and lower immune response shows promise for developing efficient mRNA vaccines with reduced side effects (Berger et al., 2024).

Although knowledge of the specific mechanisms contributing to the reagents' inflammatory effects are currently underdeveloped, it is possible that activation of PRRs contribute to a triggered immune response (Tahtinen et al., 2022). Previous studies have displayed that transfection reagents themselves are known to cause cellular stress, which may contribute to the release of IL-1α inflammatory cytokines (Komine et al., 2016).

Limitations

A significant methodological limitation of this study was the loss of RPL37A endogenous control data due to possible sample contamination. Without a reliable reference gene to normalize the input cDNA and DNA concentrations across samples, exact quantitative fold-changes in cytokine expression could not be calculated conclusively. RPL37A is a control gene that has a set number of cycles needed to amplify above the baseline phase, regardless of cell stimuli. Therefore, our cytokine data was analyzed against the fixed threshold Cq = 20, which is consistent with existing literature (Poremba, 2014). Therefore, the resulting fold-change values must be interpreted as semi-quantitative trends rather than absolute, progressive biological quantification. Future studies must ensure proper amplification of a reference gene to allow for accurate quantification.

We were also unable to investigate the exact chemistry of Lipofectamine 2000 to explain the data, as this LNP is proprietary and its product information is not publicly available. As a result, a direct structure relationship analysis was not possible. While we can conclude that specific reagents produce varying degrees of innate immune activation, we cannot pinpoint the specific molecular groups that were responsible for triggering the inflammasome pathway.

We also faced physiological constraints by relying exclusively on an *in vitro* monoculture of H1299 human lung epithelial cells. This is a widely utilized model for non-small cell lung carcinoma, but presents inherent limitations when attempting to replicate the behavior of human tissue. Additionally, it is notably p53-null, meaning it does not express any p53 tumor suppressor gene. This causes it to be vastly different from healthy human cells, potentially altering the generalizability of the results. Furthermore, utilizing a two-dimensional *in vitro* cell line fails to represent the microenvironment found in the human body. Reagents like Lipofectamine 2000 and PEI often act as adjuvants that recruit macrophages and trigger adaptive immune responses (such as T-cell activation), which can not be fully captured by this isolated system (Siebart et al., 2024).

Finally, the experimental scope of this experiment was relatively narrow, as only two transfection carriers, Lipofectamine 2000 and PEI, were measured. Additionally, the experimental design evaluated H1299 cells at a single 24-hour timepoint. Because cellular toxicity and cytokine production are both highly dose- and time-dependent variables, it is possible that the complete immune response was not fully captured. Early-response cytokines, especially the IL-1 cytokines measured in this experiment, could often peak well before 24 hours, meaning the full magnitude of the initial inflammatory response may have been missed.

Future Directions

While this data is suggestive of the superiority of the Lipofectamine 2000 LNP in being the most efficient at transfecting DNA with the smallest cytokine response, it is imperative that

future studies focus on other common laboratory transfection reagents, such as FuGENE and LyoVec, to expand the scope of the study's results. Moreover, future studies can achieve greater physiological accuracy by conducting experiments on whole tissues and model organisms rather than single cell lines. For instance, the cell line HEK-293T has been utilized in previous research to model immune response in the development of mRNA vaccine technologies (Liu et al., 2026; Warga et al., 2023). These organisms will be able to shed light on other symptoms and effects of specific lipid reagents, allowing for the modeling of the entire immune response. Once further insight is gained as to which LNPs confer the highest transfection efficiencies in *in vivo* or *ex vivo* models, research can be conducted in human models as well.

To gain further insight on the specific mechanisms for how the LNPs react to the cells in which they are introduced, further assays must be conducted to evaluate whether NLRP3, a PRR, is implicated, and to which LNPs it is activated in response to. Tahtinen et al.'s previous study aimed to understand the role of NLRP3 in LNP-associated inflammation, and further studies are needed to confirm and expand upon their findings. Future research could also explore the lipids' roles in other immune pathways to identify any underlying PRRs causing lipid-induced innate immune activation.

Our study specifically focused on the IL-1 axis (IL-1α and IL-1ß) due to its established role in LNP inflammation (Tahtinen et al., 2022). However, expression levels of IL-1RN were not studied, obscuring the complete innate immune response with regards to IL-1 cytokines. In order to broaden our characterization of how lipids affect the immune response, other key inflammatory mediators, including IFN-γ, tumor necrosis factor-α (TNF-α), IL-17A, and the chemokines CXCL8, CXCL10, and CXCL13, could be incorporated in future studies (Tahtinen et al., 2022, Warga et al., 2023). A broader cytokine and chemokine panel would determine whether differences observed in IL-1 signaling extend to other inflammatory pathways. This future study, however, must come at the result of research pertaining to PRRs and which specific, perhaps undiscovered, PRRs produce certain significant cytokines.

The present study evaluated each transfection reagent using a single reagent concentration and amount of DNA. Therefore, each reagent was only evaluated under one specific set of conditions which may not be its optimal performance range. Future studies should investigate a multitude of reagent-to-DNA ratios in order to determine which variation of this ratio will produce the largest transfection efficiency while still emitting little-to-no cytokine production as a result of the lipid itself.

**ACKNOWLEDGEMENTS**

We thank Drew University for generously hosting the Governor's School of New Jersey Program in the Sciences (GSNJS) and providing materials and facilities for the operation of this project. We would like to extend our gratitude to the sponsors of GSNJS, including Bristol Myers Squibb, The Garden State Initiative, Overdeck Family Foundation, Novartis Pharmaceuticals Corp., State of NJ: Office of the Secretary of Higher Education, BASF Environmental Catalyst and Metal Solutions, and alumni and parents who have all made this opportunity possible. We especially recognize Dr. Adam Cassano, Dr. Stephen Dunaway, Ms. Yumi Kouh, the GSNJS counselors, and all other Drew University faculty and staff who have guided us through a broad

range of scientific exploration. We are particularly grateful for counselors Brenna Hezel and Emily Shirk, who have provided us with support both within our lab procedures and throughout the progression of our research. Finally, we would like to express our immense appreciation for the invaluable guidance of Dr. Brianne Barker, our project advisors. Our journey is attributed to her boundless knowledge and unwavering belief in our abilities.

**REFERENCES**

Barber, G. STING: infection, inflammation and cancer. Nat Rev Immunol 15, 760–770 (2015). https://doi.org/10.1038/nri3921

Blakney, A. K., Top, K. A., Cowling, B. J., Larson, H. J., Shattock, R. J., & Sadarangani, M. (2026). Safety and efficacy of mRNA vaccines: A mechanistic and public health perspective. *The Lancet*. Advance online publication. https://doi.org/10.1016/S0140-6736(26)00512-X

Berger, S., Zeyn, Y., Wagner, E., & Bros, M. (2024). New insights for the development of efficient DNA vaccines. *Microbial Biotechnology*, *17*(11). https://doi.org/10.1111/1751-7915.70053

Castaño, D., Bettini, E., Kumar, B., Chudnovskiy, A., Siv, A., Protti, G., Nakadakari-Higa, S., Ceglia, S., De Luna, N., Chiu, J. E., Lederer, K., Li, S. H., Ibrahim, H., Muramatsu, H., Mdluli, T., Abraham, E., Sahingur, S. E., Maillard, I., Tam, Y. K., . . . Locci, M. (2025). Distinct components of mRNA vaccines cooperate to instruct efficient germinal center responses. *Cell*, *188*, 7461–7480. https://doi.org/10.1016/j.cell.2025.11.023

Gasteiger, G., Rudensky, A. Interactions between innate and adaptive lymphocytes. Nat Rev Immunol 14, 631–639 (2014). https://doi.org/10.1038/nri3726

Liu, Z., Zhou, J., Gao, R., Wang, Y., Liu, M., Wang, W., Wang, Y., Wei, P., Zhou, K., Wang, M., Pan, S., Xing, L., Zhang, G., Xu, W., Wang, Q., Jiang, X., Zhang, J., Zhang, Y., Zhang, Y., . . . Lu, L. (2026). Precision-engineered STING agonist nanoparticles enable coordinated mucosal-systemic immunity for durable pan-β-coronavirus protection. *Nature Nanotechnology*. Advance online publication. https://doi.org/10.1038/s41565-026-02188-z

Livak, K. J., & Schmittgen, T. D. (2001). Analysis of Relative Gene Expression Data Using Real-Time Quantitative PCR and the 2−ΔΔCT Method. Methods, 25(4), 402–408. https://doi.org/https://doi.org/10.1006/meth.2001.1262

Locci, M., & Pardi, N. (2026). Immunological mechanisms of mRNA vaccines for infectious diseases. *Nature*, *654*, 892–901. https://doi.org/10.1038/s41586-026-10599-0

Malewana, R. D., & Corbett-Helaire, K. S. (2026). The dual-adjuvant logic of mRNA vaccines. *Trends in Immunology*, *47*(4), 243–245. https://doi.org/10.1016/j.it.2026.01.012

Mantovani, A., Dinarello, C. A., Molgora, M., & Garlanda, C. (2019). IL-1 and related cytokines in innate and adaptive immunity in health and disease. *Immunity*, *50*(4), 778–795. https://doi.org/10.1016/j.immuni.2019.03.012

Poremba, C., Uhlendorff, J., Pfitzner, B. M., Hennig, G., Bohmann, K., Bojar, H., Krenn, V., Brase, J. C., Haufe, F., Averdick, M., Dietel, M., Kronenwett, R., & Denkert, C. (2014). Preanalytical variables and performance of diagnostic RNA-based gene expression analysis in breast cancer. *Virchows Archiv : an international journal of pathology*, *465*(4), 409–417. https://doi.org/10.1007/s00428-014-1652-0

Tahtinen, S., Tong, A.-J., Himmels, P., Oh, J., Paler-Martinez, A., Kim, L., Wichner, S., Oei, Y., McCarron, M. J., Freund, E. C., Amir, Z. A., de la Cruz, C. C., Haley, B., Blanchette, C., Schartner, J. M., Ye, W., Yadav, M., Sahin, U., Delamarre, L., & Mellman, I. (2022). IL-1 and IL-1ra are key regulators of the inflammatory response to RNA vaccines. *Nature Immunology, 23*(4), 532–542. https://doi.org/10.1038/s41590-022-01160-y

Thakur, G., Mink, S., Bak, H., & Tustian, A. D. (2024). Improving process efficiency to reduce cost-of-goods per dose in manufacturing of recombinant AAVs. *Cell & Gene Therapy Insights*, *10*(3), 479–499. https://doi.org/10.18609/cgti.2024.061

Rehman, K., Afzaal, A., Sajid Hamid Akash, M., Imran, M., & A. Assiri, M. (2023). Interleukin-1 receptor antagonist: From synthesis to therapeutic applications. *Biocell*, *47*(4), 809–823. https://doi.org/10.32604/biocell.2023.025850

Tsaregorodtseva, T. S., Radyukhina, M. A., Ayupova, A. I., Solovyeva, V. V., Sufianov, A. A., Sufianova, G. Z., & Rizvanov, A. A. (2026). Safety of adeno-associated viral vectors in gene therapy: Mechanisms of toxicity, clinical risks, and strategies for their minimization. *International Journal of Molecular Sciences*, *27*(11), Article 4818. https://doi.org/10.3390/ijms27114818

Warga, E., Anderson, J., Tucker, M., Harris, E., & Elmer, J. (2023). Transcriptomic analysis of the innate immune response to in vitro transfection of plasmid DNA. *Molecular Therapy — Nucleic Acids, 31*, 43–56. https://doi.org/10.1016/j.omtn.2022.11.025

Wei, C., Zhu, Y., Lu, X. et al. Lipid nanoparticle composition directs systemic trafficking and tissue-specific T cell immunity after intramuscular injection. Nat. Biomed. Eng (2026). https://doi.org/10.1038/s41551-026-01706-7

**APPENDIX**

Abbreviations

1. IL-1: Interleukin-1
2. IL-1α: Interleukin-1 alpha
3. IL-1β: Interleukin-1 beta
4. IL-1ra: Interleukin-1 receptor antagonist
5. IL-1R1: Interleukin-1 receptor type 1
6. IL-2: Interleukin-2
7. IL-6: Interleukin-6
8. IL-17A: Interleukin-17A
9. TNF/TNF-α: Tumor necrosis factor/tumor necrosis factor alpha
10. IFN-γ: Interferon gamma
11. CXCL8, CXCL10, CXCL13: Motif chemokine ligand 8, 10, and 13
12. NF-κB: Nuclear factor kappa-light-chain-enhancer of activated B cells
13. PRR(s): Pattern recognition receptor(s)
14. cGAS: Cyclic GMP (guanosine monophosphate) - AMP (adenosine monophosphate) synthase
15. STING: Stimulator of interferon genes
16. IFI16: Interferon-inducible protein 16
17. TLR7/TLR8: Toll-like receptor 7/Toll-like receptor 8
18. NLRP3: nucleotide-binding oligomerization domain-like receptor protein 3
19. CD8+: Cluster of differentiation 8-positive

20. Tfh: T follicular helper
21. DC: Dendritic cell
22. DNA: Deoxyribonucleic acid
23. RNA: Ribonucleic acid
24. mRNA: Messenger ribonucleic acid
25. GFP: Green fluorescent protein
26. qPCR: Quantitative polymerase chain reaction
27. *ampR*: Ampicillin resistance
28. RNA-LPX: ribonucleic acid-lipoplex
29. HEK293T: Human embryonic kidney 293 cells
30. DMEM: Dulbecco's modified eagle medium
31. PEI: Polyethylenimine
32. $CO_2$: Carbon dioxide
33. kL: Kiloliter
34. PEG: Polyethylene glycol
35. Cy5: Cyanine 5
36. COVID-19: Coronavirus disease 2019
37. AAV: Adeno-associated virus
38. LNP: Lipid nanoparticle
39. MDN: Moderna COVID-19 vaccine formulation
40. PBT: Pfizer-BioNTech vaccine formulation
41. ALN: Alnylam Onpattro formulation
42. DMG-PEG2000: dimyristoylglycerol polyethylene glycol 2000
43. DI-8: SEE CD8+
44. Opti: Opti-MEM media
45. DNA solution: (6.25 ng/µL) pcDNA3-EGFP solution